Ion-Beam Focusing in a Double-Plasma Device

JAMES C. JOHNSON, NICOLA D'ANGELO, AND ROBERT L. MERLINO

Abstract—**We have studied the propagation of a low-energy, charge-neutralized ion beam which is injected into the target region of a long double-plasma (DP) device. A magnetic field of up to ~180 G may be applied along the axis of the device. As a result of charge exchange collisions, the ion beam is attenuated as it propagates into the target region. However, under certain conditions of magnetic field strength and neutral gas pressure, we have observed a "reemergence" of the beam on axis far downstream in the target. This reemergence of the ion beam is attributed to a focusing of the ions by a self-consistently produced radial ambipolar electric field. The effect may be expected to occur in other types of plasma devices as well, whenever a sufficiently large radially inward electric field is present.**

I. Introduction

DOUBLE-PLASMA (DP) devices have been in use for a number of years. They are well suited to the study of the interaction of an ion beam of variable energy with a background plasma [1]–[3]. Only recently has a longitudinal magnetic field been added to such devices, as in Merlino and D'Angelo [4] and in Pierre *et al.* [5]. The addition of a longitudinal magnetic field of ~100 G or more near the center plane of the device requires that the hot filaments of the driver and of the target chambers be located in the fringing field regions at either end so that density filamentation may be avoided. This particular arrangement, however, may be in part responsible for a phenomenon that we have observed recently and which is discussed in the present paper.

Our magnetized DP device, which was recently put into operation and is described in Section II, is largely intended for studies of wakes from objects of various sizes and shapes, when the objects are immersed in supersonic plasma flows of various Mach numbers. As a preliminary investigation, it was necessary to examine in some detail the behavior of ion beams injected into the target chamber when no object or obstacle of any kind was present there. This was done by means of ion-energy analyzers of the type we have often used in the past, e.g., Merlino and D'Angelo [4] and Cartier *et al.* [6]. As expected, we found that an ion beam, as it travels axially into the target, is attenuated by charge-exchange collisions with neutral gas (argon) atoms, e.g., D'Angelo [3]. However, under suitable combinations of gas pressure and magnetic field strength a "reemergence" of the beam on axis may occur far downstream in the target. The reemergence effect is apparently produced by a focusing of those beam ions which are initially injected at the outer portions of the plasma column. These ions are acted upon by an electric field of ~0.1 V/cm, directed everywhere radially inward and self-consistently produced, for appropriate values of the neutral pressure and of the magnetic field, by a faster intrinsic outward diffusion of the plasma ions relative to that of the electrons.

In Section II we describe the magnetized DP device in which the experiments were performed. In Section III some of the initial data are presented that made the ion-beam reemergence effect apparent. Section IV shows how radially inward electric fields of sufficient magnitude to produce beam focusing can, in fact, arise under appropriate conditions. Section V presents the experimental data we have obtained in order to verify the predictions of Section IV. Finally, Section VI contains the conclusions.

II. The Magnetized Double-Plasma (DP) Device

A schematic diagram of the DP device is shown in Fig. 1(a), while Fig. 1(b) shows the axial profile of the longitudinal magnetic field (on axis). As can be seen from Fig. 1, the magnetic field is quite uniform in the central region of the device, over a distance of approximately 160 cm, but decreases very rapidly as one enters either end chamber. The maximum magnetic field strength available near the center plane is ~180 G.

Plasma is produced in the end chambers by primary electrons emitted from hot tungsten filaments, which are biased at ~ −40 V relative to the walls of either chamber. The primary electrons ionize the neutral (argon) gas which fills the device at a pressure in the $\sim 5 \times 10^{-5}$ torr to $\sim 5 \times 10^{-4}$ torr range (the base pressure is 1×10^{-6} torr or less). The plasma density is, generally, 10^9 cm^{-3} to 10^{10} cm^{-3}. Electron and ion temperatures in DP devices are, typically, $T_e \sim$ 1–2 eV and $T_i \sim$ 0.2–0.3 eV.

The driver and target plasmas are separated by a grid, which is held at a voltage of −75 V to prevent the primary electrons of either chamber from entering the other. By biasing at a suitable positive voltage the walls of the driver, an ion beam is injected from the driver into the target.

Measurements of plasma density and density fluctuations are performed by means of Langmuir probes. Emissive probes are used for measurements of the space potential. Ion beams injected from the driver into the target are detected by means of electrostatic retarding potential analyzers, consisting of two grids and a collector, of the type described in Merlino and D'Angelo [4] and in

Manuscript received April 18, 1988; revised June 10, 1988. This work was supported by the ONR and NASA.

The authors are with the Department of Physics and Astronomy, University of Iowa, Iowa City, IA 52242.

IEEE Log Number 8823061.

0093-3813/88/1000-0590$01.00 © 1988 IEEE

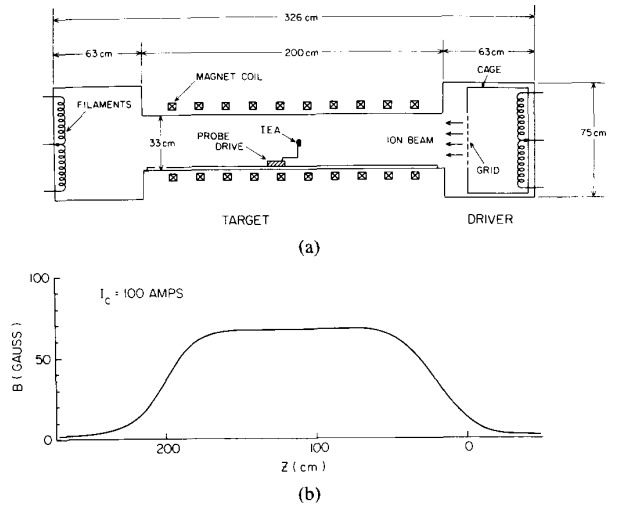

Fig. 1. (a) A schematic of the double-plasma device used in this study. The ion energy analyzer (IEA) is mounted on a probe drive which can move over an axial distance of 160 cm and make transverse (radial) scans of the plasma column. (b) The axial magnetic field profile for a total current supplied to the coils of 100 A.

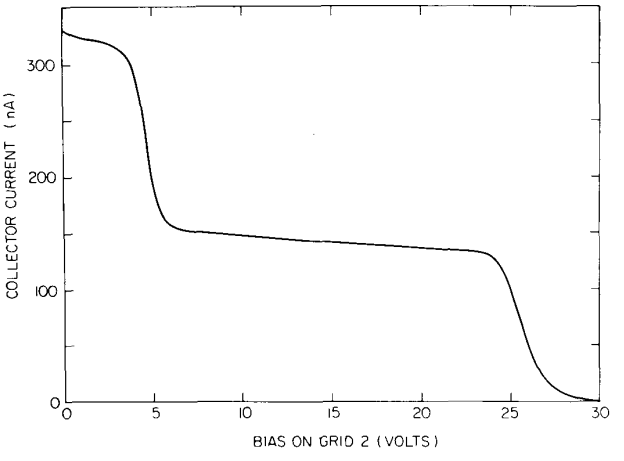

Fig. 2. A typical ion-energy analyzer curve of collector current versus retarding grid voltage.

Cartier *et al.* [6]. A typical analyzer curve is shown in Fig. 2. In addition to Langmuir probes and ion-energy analyzers which can be inserted into the plasma column from side ports of the target chamber, and which can be moved radially across the column at fixed axial positions, the DP device is also provided with a probe/analyzer drive system capable of taking radial plasma/beam scans at any axial location within the central region of the device, where the magnetic field is uniform. The axial motion of the drive system extends over a region 160 cm long.

III. The Phenomenon of Ion-Beam Reemergence

As noted in the Introduction, axial ion-beam intensity profiles always showed the intensity decrease with the increase of distance into the target expected from charge exchange with the argon atoms present in the device.

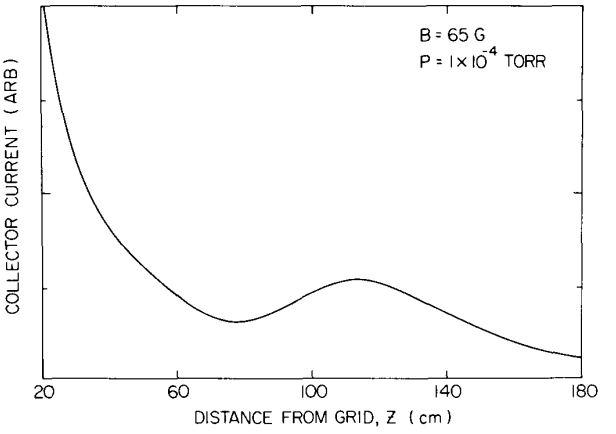

Fig. 3. Axial profile of the ion-beam intensity (collector current) showing the beam "reemergence" effect.

However, under appropriate conditions of gas pressure and magnetic field intensity, an axial reemergence of the beam was observed further downstream. An example of this phenomenon is shown in Fig. 3. This axial profile of the beam intensity was taken by biasing the analyzer grid of the ion-energy analyzer at a fixed voltage, large enough (v_g = 12.4 V) to exclude the plasma ions but small enough to accept all the beam ions. The argon pressure was 1×10^{-4} torr and the magnetic field strength near the mid-plane was 65 G. Since the effect shown in Fig. 3 was observed several times for other pressure/magnetic field combinations, an explanation of this phenomenon was required.

It might appear at first sight that the beam reemergence could be caused by a charge exchange of energetic neutral atoms formed by previous charge exchanges of beam ions with argon atoms. However, we discarded this possibility for two reasons. In the first place, it is not clear why a reionization of fast neutrals should give rise to an intensity *peak*, like the one located at $\simeq$123 cm in Fig. 3, rather than to a monotonic variation of the intensity with increasing axial distance. In the second place, the mean free path for a charge exchange of a fast neutral atom in a plasma of density $n \approx 10^{10}$ cm^{-3} is $\lambda \sim 1/\sigma n \sim 10^4$ cm, if we assume a charge-exchange cross section, σ, of $\sim 10^{-14}$ cm^2. Thus, λ is much too large compared to the length of the device for the effect to be important. The argument, of course, becomes even more cogent if the plasma density is smaller than 10^{10} cm^{-3}.

A second possibility that we considered was that, somehow, in the presence of a magnetic field the sheath formation at the grid separating driver and target chambers might be affected in such a way as to provide, in the target plasma immediately adjacent to the grid, electric fields with radial components directed inward, toward the axis of the device. These fields could then focus the ions crossing the grid near its outer rim. However, a simple argument showed that this possibility had also to be discarded. The Debye length near the grid is $\lambda_D \sim 10^{-2}$ cm, while the electron and ion gyroradii are $\rho_e \sim 1$ cm and $\rho_i \sim 1$

m, respectively. Since both ρ_e and ρ_i are much larger than the Debye length, it is hard to see how the sheath formation at the grid, and thus the electric fields there, could be affected by the presence of the magnetic field.

Having thus discarded the above two possibilities, we examined a third one which is dealt with in Section IV. It also relies on a focusing of beam ions by electric fields. However, in this case the electric fields are present all along the plasma column and are produced by the different intrinsic rates of diffusion transverse to $\boldsymbol{B}$ of plasma ions and electrons. It appears that these $\boldsymbol{E}$ fields are indeed capable of focusing the beam ions and of producing the effect shown in Fig. 3. Section V presents data which support this focusing mechanism.

IV. Radial $\boldsymbol{E}$ Fields and Ion-Beam Focusing

We show in this section: first, how the radial electric fields in a partially ionized plasma column depend, in both magnitude and sign, on the neutral pressure and on the magnetic field strength, and secondly, how inward fields might be responsible for the reemergence phenomenon of Section III through beam focusing. The calculations are done for the case of a uniform magnetic field. This is not the case in our DP device except over a distance of ~ 160 cm near the central plane. However, the results that we obtain are applicable to our experiment, provided the value of $\boldsymbol{B}$ assumed in the calculations represents a suitable axial average of the magnetic field in the device.

In a steady-state situation, with both the ion and the electron inertial terms $(\boldsymbol{v} \cdot \nabla \boldsymbol{v})$ neglected, the ion and the electron momentum equations read

$$\begin{aligned} \kappa T_i \nabla \boldsymbol{n} - en\boldsymbol{E} - en\boldsymbol{v}_i \times \boldsymbol{B} &= -\nu_i n m_i \boldsymbol{v}_i \\ \kappa T_e \nabla \boldsymbol{n} + en\boldsymbol{E} + en\boldsymbol{v}_e \times \boldsymbol{B} &= -\nu_e n m_e \boldsymbol{v}_e \end{aligned} \tag{1}$$

with the usual meaning of the various symbols. The terms $-\nu_i n m_i \boldsymbol{v}_i$ and $-\nu_e n m_e \boldsymbol{v}_e$ represent momentum losses by the ions and the electrons, respectively, due to collisions with the neutral gas atoms.

By taking components of (1), one finds for the radial velocity of the plasma ions and electrons:

$$\begin{aligned} v_{ir} &= -\frac{1}{\nu_i m_i (1 + \omega_{ci}^2/\nu_i^2)} \left\{ \kappa T_i \frac{1}{n}\frac{dn}{dr} - eE \right\} \\ v_{er} &= -\frac{1}{\nu_e m_e (1 + \omega_{ce}^2/\nu_e^2)} \left\{ \kappa T_e \frac{1}{n}\frac{dn}{dr} + eE \right\} \end{aligned} \tag{2}$$

where ω_{ci} and ω_{ce} are the ion and electron gyrofrequency, respectively.

Next, we impose the condition that $v_{ir} = v_{er}$, as must be the case in a steady-state situation in which the rates of production per unit volume of ions and electrons are the same. This condition determines the magnitude and the sign of the $\boldsymbol{E}$ field that must self-consistently arise to ensure equal radial losses for ions and electrons. We obtain

$$E = \left[\frac{\dfrac{\omega_{ci}/\nu_i}{1 + \omega_{ci}^2/\nu_i^2}\dfrac{\kappa T_i}{e} - \dfrac{\omega_{ce}/\nu_e}{1 + \omega_{ce}^2/\nu_e^2}\dfrac{\kappa T_e}{e}}{\dfrac{\omega_{ci}/\nu_i}{1 + \omega_{ci}^2/\nu_i^2} + \dfrac{\omega_{ce}/\nu_e}{1 + \omega_{ce}^2/\omega_e^2}} \right] \cdot \left(\frac{1}{n}\frac{dn}{dr} \right). \tag{3}$$

If $\kappa T_i/e$ and $\kappa T_e/e$ are expressed in volts and $(1/n)(dn/dr)$ in cm^{-1}, the E field is expressed in V/cm. Note that for a given T_i, T_e, and $(1/n)(dn/dr)$, the $\boldsymbol{E}$ field is entirely determined by ω_{ci}/ν_i and ω_{ce}/ν_e. Since both ω_{ci}/ν_i and ω_{ce}/ν_e are proportional to the ratio B/p between the magnetic field strength and the neutral gas pressure, the $\boldsymbol{E}$ field is determined in sign and magnitude by the parameter B/p.

We have calculated the $\boldsymbol{E}$ field given by (3) for several values of B, p, T_i, T_e, assuming cross sections for electron–atom and argon ion–atom collisions $\sigma_{en} = 5 \times 10^{-16}$ cm^2 and $\sigma_{in} = 1 \times 10^{-14}$ cm^2, respectively.

Fig. 4 shows the coefficient, A, of $(1/n)(dn/dr)$ in (3), for $\kappa T_i = 0.3$ eV, $\kappa T_e = 1.5$ eV, and a neutral gas pressure of 4×10^{-4} torr. The magnetic field intensity is varied in this case from 10^{-1} G to 10 G. Since $(1/n)(dn/dr) < 0$, positive A's correspond to negative E fields, i.e., to situations in which the outer portions of the plasma column are more positive than regions near the axis. Negative values of A correspond to situations with the outer portions more negative. In the case of Fig. 4, only for $B \gtrsim 2.3$ G is A positive. This dependence of A on B is evidently related to the fact that, for the larger $\boldsymbol{B}$ fields, the electrons are essentially magnetized, while the plasma ions can diffuse more easily outward through ion–neutral collisions. For the smaller $\boldsymbol{B}$ fields, both ions and electrons are essentially unmagnetized, and the electrons tend to escape faster than the ions can.

Fig. 5 presents similar calculations for $\kappa T_i = 0.3$ eV, $\kappa T_e = 1.5$ eV, and several values of the natural gas pressure, from 5×10^{-5} torr to 8×10^{-4} torr. The B field in this figure varies from 10^{-1} G to 100 G. As can be seen from this figure, as the neutral gas pressure increases the magnetic field at which the transition occurs between positive and negative A (i.e., $A = 0$) also increases. This is illustrated in Fig. 6, which shows, as a function of B, the neutral gas pressure at which A, and thus the radial $\boldsymbol{E}$ field, is zero. To the right of the line we have $E < 0$, corresponding to a plasma column with the outer regions at a more positive potential than the regions near axis. As far as the magnitude of the self-consistent $\boldsymbol{E}$ field is concerned, Fig. 5 indicates that, for 0.5×10^{-5} torr $\leq p \leq 8 \times 10^{-4}$ torr and $B \gtrsim 15$ G, the magnitude of A is ~ 0.3 V. If the e-folding length of the radial density profile is

$$\left(\frac{1}{n}\frac{dn}{dr} \right)^{-1} \approx 3 \text{ cm}$$

we obtain in this case an inward electric field $E \simeq 0.1$ V/cm.

Fields of comparable magnitudes were observed in a

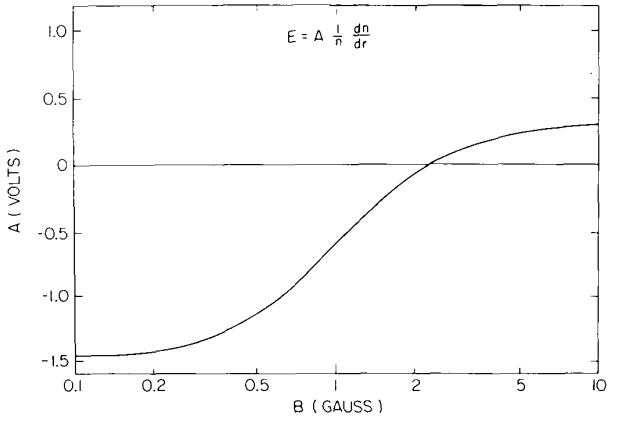

Fig. 4. The coefficient, A, of $(1/n)(dn/dr)$ in equation (3) as a function of magnetic field strength for $T_i = 0.3$ eV, $T_e = 1.5$ eV, $p = 4 \times 10^{-4}$ torr, and using ion-neutral and electron-neutral collision cross sections of 1×10^{-14} cm^2 and 5×10^{-16} cm^2, respectively.

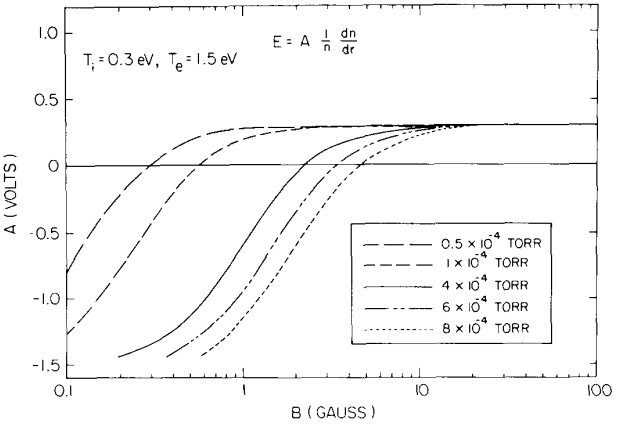

Fig. 5. The coefficient, A, of $(1/n)(dn/dr)$ versus magnetic field strength for the same conditions as in Fig. 4, for five different pressures.

magnetized DP device similar to the present one by Merlino and D'Angelo [4], who also observed at a fixed pressure of 3×10^{-5} torr the expected transition from positive to negative radial E field, as the strength of the magnetic field was varied. Additional data of the same type, taken in the present DP device, are presented also in Section V.

We discuss next the focusing effects of radially inward $\boldsymbol{E}$ fields. If the beam reemergence of Section III is indeed due to a focusing of ions toward the axis by the negative (i.e., inward) radial $\boldsymbol{E}$ field in the column, we should expect this phenomenon to occur at any given pressure only when the $\boldsymbol{B}$ field is strong enough to make A positive. Also, as p is varied, the minimum $\boldsymbol{B}$ field required to observe focusing should change as indicated in Fig. 6.

Assume now that a radially inward $\boldsymbol{E}$ field is present over the entire length of the column, with an average intensity E. An ion injected at the grid with an axial velocity

$$v_0 = \left(\frac{2eV_b}{m}\right)^{1/2}$$

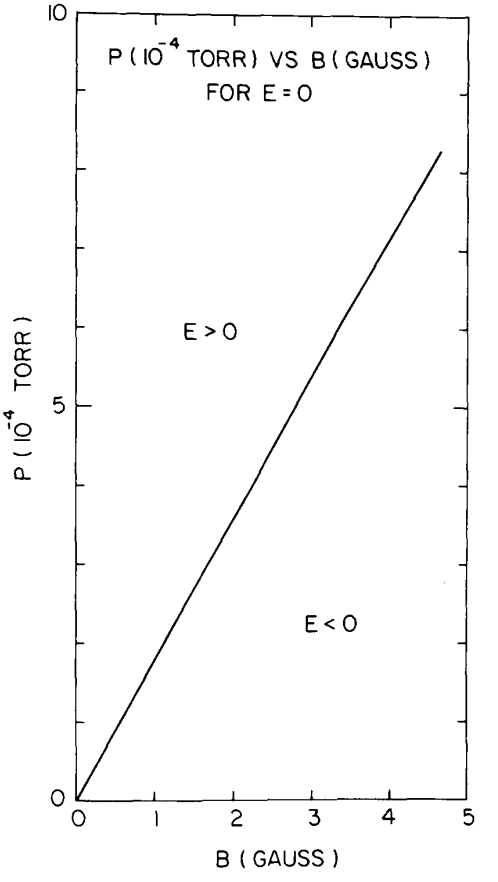

Fig. 6. The neutral pressure for which the radial electric field vanishes versus B.

where eV_b is the beam energy, will be displaced radially inward by an amount, r_0, after traveling an axial distance z^* downstream, given by

$$z^* = 2\,\frac{r_0^{1/2} V_b^{1/2}}{E^{1/2}}. \tag{4}$$

If we take $r_0 = 10$ cm, $V_b = 20$ V, and $E = 0.1$ V/cm, we find $z^* \simeq 90$ cm. This indicates that the strength of the expected radial $\boldsymbol{E}$ field is large enough to produce substantial focusing of the beam ions over distances comparable to those over which the reemergence effect of Section III is observed.

Data taken to examine this focusing mechanism are presented in Section V.

V. Experimental Results

In this section we present experimental results obtained in order to test the focusing mechanism discussed in Section IV.

Fig. 7 shows plots of the ion-beam intensity versus axial distance away from the grid separating driver and target for a value of the magnetic field at the center plane of the DP device of 20 G and for four different values of the neutral gas pressure. In all four cases the beam intensity

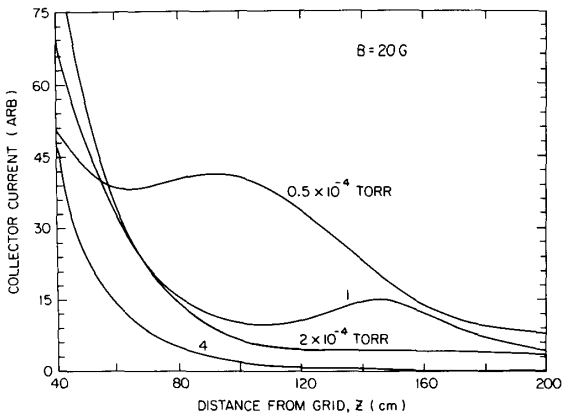

Fig. 7. Axial profiles of the ion-beam intensity for four different neutral pressures. The B field is 20 G and the beam energy, 12.5 eV.

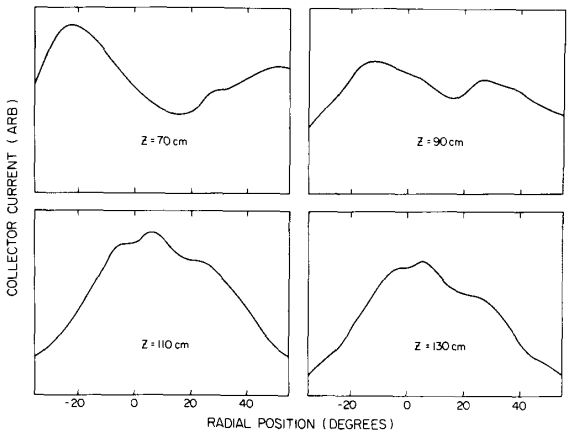

Fig. 8. Radial profiles of the ion-beam intensity for distances from the grid of 70, 90, 110, and 130 cm (beam energy of 10 eV, pressure of 1×10^{-4} torr, and magnetic field of 65 G). A $\Delta\theta = 10°$ corresponds to a radial distance of ~2.6 cm.

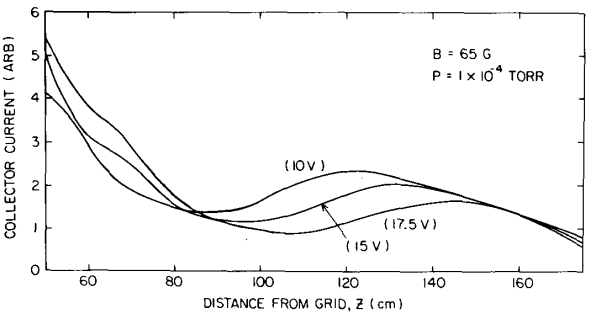

Fig. 9. Axial profiles of the ion-beam intensity for three different beam energies ($p = 1 \times 10^{-4}$ torr, $B = 65$ G).

decreases, monotonically at first, with distance away from the grid. However, for the lowest two pressures of 5×10^{-5} torr and 1×10^{-4} torr, the beam is clearly seen to reemerge. This reemergence of the beam, on the other hand, is not seen for the largest pressure of 4×10^{-4} torr. This result is evidently in general agreement with the predictions of Fig. 6, giving, for each $\boldsymbol{B}$ field, the neutral pressure below which beam reemergence is expected. A precise quantitative comparison of the experimental results with the computations is difficult for at least two reasons. In the first place, the $\boldsymbol{B}$ field in the experiments is nonuniform between the grid and, say, $z \approx 60$ cm, so that for a proper comparison with the calculations some average of the $\boldsymbol{B}$ field over the region of nonuniformity would have to be taken. In the second place, the computations leading to Fig. 6 assume certain values for the cross sections for momentum exchange of electrons with neutrals and of ions with neutrals. These cross sections could be in error by factors of two or so. In addition, the assumption of a rather uniform radial $\boldsymbol{E}$ field all along the column is clearly not satisfied. However, in spite of these shortcomings in the comparison of experimental data with computations, one is encouraged by the result that the existence of a "critical" pressure (for any $\boldsymbol{B}$ field) for the appearance of the beam reemergence effect is borne out by the experiment, and for values of the $\boldsymbol{B}$ field (when suitably averaged along the column) comparable to those computed.

As the next step in this line of investigation, we tried to observe directly the effect of ion-beam focusing by measuring the radial ion-beam profile at several values of z, the axial distance away from the grid. Fig. 8 shows some results of this type of measurement. Evidently, the radial intensity maxima present at $z = 70$ cm converge radially as one moves to $z = 90$ cm and blend into one single maximum at $z = 110$, 130 cm.

One further test of the mechanism discussed in Section IV consisted in observing the variation of the axial position of beam reemergence with beam energy, predicted by (4). Fig. 9 shows axial scans of the beam intensity for a pressure of 1×10^{-4} torr, a $\boldsymbol{B}$ field at mid-plane of 65 G, and three different values of the beam energy. Evidently, as the beam energy is increased the axial intensity maximum is displaced to larger and larger z's. Equation (4) predicts a linear dependence of the axial distance, z^*, of the intensity maximum on the square root of the beam energy, $z^* \propto V_b^{1/2}$. The observed relation between z^* and $V_b^{1/2}$ is shown in Fig. 10.

Finally, the dependence of the radial $\boldsymbol{E}$ field in the plasma on pressure and the magnetic field was investigated. Fig. 11 shows radial potential profiles, measured with an emissive probe, at a pressure $p = 3 \times 10^{-4}$ torr and for several values of the magnetic field. From this figure, for $B \approx 20$–60 G, a radial inward $\boldsymbol{E}$ on the order of 0.1 V/cm is easily inferred, in agreement with Section IV.

Similar data, obtained at various neutral gas pressures, were used to construct the solid line in Fig. 12, which shows the neutral gas pressure as a function of $\boldsymbol{B}$ for which the positive–negative $\boldsymbol{E}$ field transition is observed ($E =$

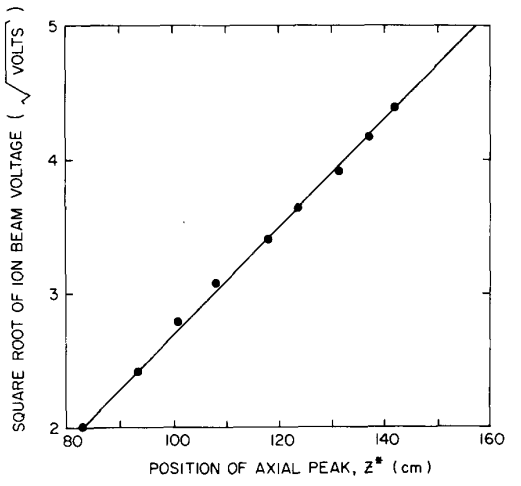

Fig. 10. Square root of the ion-beam voltage versus position of the axial peak, determined from plots similar to those of Fig. 9, but with a magnetic field of 80 G.

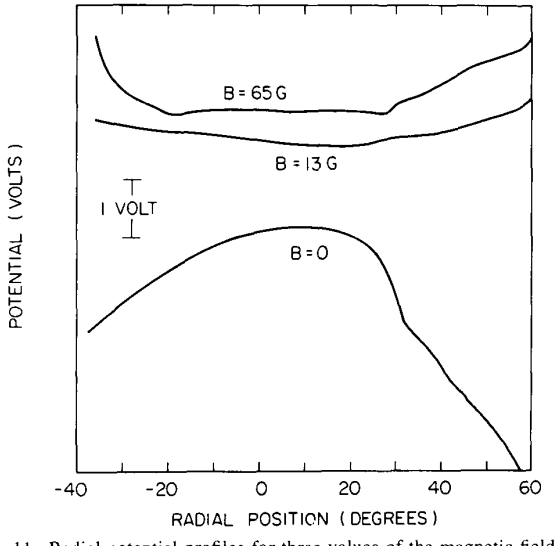

Fig. 11. Radial potential profiles for three values of the magnetic field at $z = 100$ cm and for $p = 3 \times 10^{-4}$ torr. The curves have been displayed vertically for clarity. A $\Delta\theta = 10°$ corresponds to a radial distance of ~ 2.6 cm.

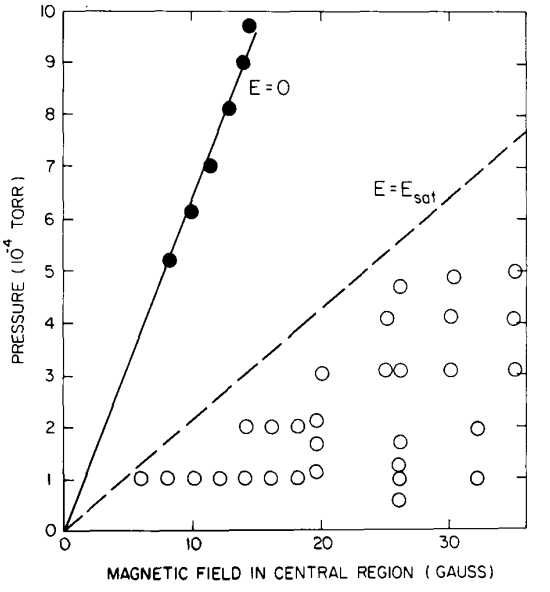

Fig. 12. The solid line shows the neutral gas pressure as a function of $\boldsymbol{B}$ for which $E = 0$, as determined from data similar to those of Fig. 11. The dashed line has a slope of one-third that of the solid line (see text). The circles (○) denote p, $\boldsymbol{B}$ pairs for which beam reemergence has been observed.

0). Examination of Fig. 5 shows that for each gas pressure the $\boldsymbol{B}$ field, at which a negative "saturation" $\boldsymbol{E}$ field is attained, is about three times as large as the $\boldsymbol{B}$ field at which $\boldsymbol{E} = 0$. The dashed line ($\boldsymbol{E} = \boldsymbol{E}_{sat}$) in Fig. 12 has been drawn with a slope equal to one-third of that of the solid line ($\boldsymbol{E} = 0$). In the same figure we have marked, for several p, $\boldsymbol{B}$ pairs, some of the points where the beam reemergence effect was present (○). For any given pressure, the reemergence of the beam was definitely observed only for values of the magnetic field to the right of the dashed line.

VI. Discussion and Conclusions

A 2 m long magnetized double-plasma (DP) device has been put into operation recently at the University of Iowa. When an ion beam is injected from the driver into the target chamber, the beam intensity is observed to decay with increasing distance away from the separation grid. This decay can be accounted for in terms of charge-exchange collisions between the beam ions and the neutral gas in the chamber. At low pressures and/or high magnetic fields, however, axial scans of the ion-beam intensity exhibit a reemergence of the ion beam, as described in Sections III and V. This phenomenon has been interpreted in terms of a focusing of the ion beam toward the axis of the device by self-consistent radial, inward electric fields of ~ 0.1 V/cm, produced by the faster intrinsic rate of radial diffusion of the plasma ions relative to that of the electrons. The focusing mechanism has been discussed in Section IV and experimental data supporting it have been presented in Section V.

Two questions may still be raised concerning the mechanism responsible for the beam reemergence. The first is whether a type of focusing mechanism may be operative different from that discussed in Section IV. It is conceivable that if, somehow, the ion beam were to be partially "chopped" at the grid, ion gyrations in the axial magnetic field would result in spatially periodic reenhancements of the beam intensity on axis. This mechanism would be similar to the one observed by Schmitt [7] in wake studies in a Q-machine. We think we can discard this possibility for two reasons. First of all, when we compute the axial distance for the expected first maximum we find that it should occur much further downstream than

is observed. In the second place, a mechanism of this type does not provide any easy answer as to why the beam reemergence observed in our experiments should be pressure dependent and, in particular, should depend on pressure through the B/p parameter (e.g., Fig. 12).

The second question is why we have not observed before (e.g., in Merlino and D'Angelo [4]) the effect reported here. There are two main differences between the present experimental set-up and that of [4]; namely, a) the present device is much longer, thus allowing axial beam scanning over a longer distance, and b) the grid separating driver and target chambers is located, in the present experiments, well into the region of the fringing magnetic field. This may have enhanced the focusing effect, making it easier to observe.

The phenomenon discussed in this paper may appear in other types of plasma devices as well, whenever a radially inward electric field of sufficient intensity is produced by the differential intrinsic rates of escape of plasma particles across a magnetic field.

Acknowledgment

The authors wish to thank T. Clark and A. Scheller for their expert technical assistance in the design and construction of the double-plasma device.

References

[1] R. J. Taylor, K. R. MacKenzie, and H. Ikezi, "A large double plasma device for plasma beam and wave studies," *Rev. Sci. Instr.*, vol. 43, p. 1675, 1972.
[2] R. J. Taylor and F. V. Coroniti, "Ion heating via turbulent ion acoustic waves," *Phys. Rev. Lett.*, vol. 29, p. 34, 1972.
[3] N. D'Angelo, "Ion beam scattering by ion-acoustic turbulence," *Plasma Phys.*, vol. 21, p. 973, 1979.
[4] R. L. Merlino and N. D'Angelo, "The interaction of a conducting object with a supersonic plasma flow: Ion deflection near a negatively charged obstacle," *J. Plasma Phys.*, vol. 37, p. 185, 1987.
[5] T. Pierre, G. Leclert, and F. Braun, "Magnetized double plasma device for wave studies," *Rev. Sci. Instr.*, vol. 58, p. 6, 1986.
[6] S. L. Cartier, N. D'Angelo, and R. L. Merlino, "A laboratory study of ion energization by EIC waves and subsequent upstreaming along diverging magnetic field lines," *J. Geophys. Res.*, vol. 91, p. 8025, 1986.
[7] J. P. M. Schmitt, "Wake past an obstacle in a magnetized plasma flow," *Plasma Phys.*, vol. 15, p. 677, 1973.